Increase of dissolved inorganic carbon and decrease of pH in near surface waters of the Mediterranean Sea during the past two decades

Liliane Merlivat [a], Jacqueline Boutin [a], David Antoine [b,c], Laurence Beaumont [d], Melek Golbol [c], Vincenzo Vellucci. [c]

[a] Sorbonne Université-CNRS-IRD-MNHN, LOCEAN, F-75005 Paris, France

[b] Remote Sensing and Satellite Research Group, School of Earth and Planetary Sciences, Curtin University, Perth, Australia

[c] Sorbonne Université-CNRS, Laboratoire d'Océanographie de Villefranche, LOV, F-06230 Villefranche-sur-Mer, France

[d] Division Technique INSU-CNRS, F- 92195 Meudon Cedex, France

Corresponding author: L. Merlivat (merlivat@locean.upmc.fr)

Abstract

Two 3-year time series of hourly measurements of the fugacity of CO_2 (fCO_2) in the upper 10 m of the surface layer of the northwestern Mediterranean Sea have been recorded by CARIOCA sensors almost two decades apart, in 1995-1997 and 2013-2015. By combining them with alkalinity derived from measured temperature and salinity, we calculate changes of pH and dissolved inorganic carbon (DIC). DIC increased in surface seawater by ~ 25 μmol kg^{-1} and fCO_2 by 40 μatm, whereas seawater pH decreased by ~ 0.04 (0.0022 yr^{-1}). The DIC increase is about 15% larger than expected from equilibrium with atmospheric CO_2. This could result from natural variability, e.g. the increase between the two periods in the frequency and intensity of winter convection events. Likewise, it could be the signature of the contribution of the Atlantic Ocean as a source of anthropogenic carbon to the Mediterranean Sea through the strait of Gibraltar. We then estimate that the part of DIC accumulated over the last 18 years represents ~30% of the total inventory of anthropogenic carbon in the Mediterranean Sea.

1 Introduction

The concentration of atmospheric carbon dioxide (CO_2) has been increasing rapidly over the 20th century and, as a result, the concentration of dissolved inorganic carbon (DIC) in the near surface ocean increases, which drives a decrease in pH in order to maintain a chemical equilibrium. These changes have complex direct and indirect impacts on marine organisms and ecosystems [*Gattuso and Hansson*, 2011]. Empirical methods to estimate the anthropogenic CO_2 penetration in the ocean since the industrial revolution have improved over the past few decades [*Chen and Millero*, 1979; *Gruber et al.*, 1996; *Sabine et al.*, 2008; *Touratier and Goyet*, 2004; 2009; *Woosley et al.*, 2016]. As the concentration of anthropogenic carbon, C_{ant}, cannot be distinguished from the natural background of DIC through total DIC measurements, these methods are based on the analysis of different chemical properties of the water column. Direct estimates of the anthropogenic CO_2 absorption in the sea surface layers are difficult owing to the large natural variability driven by physical and biological phenomena. Bates et al [2014] have extracted the trend from the large variability, based on analysis of a long time series (monthly or seasonal sampling). For the global surface ocean, Lauvset et al. [2015] have used the Surface Ocean CO_2 Atlas (SOCAT) database [*Bakker et al.*, 2014] combined with an interpolation method. Estimates of anthropogenic storage in the Mediterranean Sea differ by about a factor of two [*Huertas et al.*, 2009; *Touratier and Goyet*, 2009]. In addition to the anthropogenic signal, oceanic DIC can also be the signature of a strong interannual variability. In the North Atlantic, for instance, McKinley et al. [2011] have shown that the long term trend emerges only after more than 25 years because of natural variability.

A high frequency sampling of the seawater carbon chemistry at the air-water interface over extended periods of time is useful to assess trends and variability of DIC. In this paper we analyze two three-year time series of hourly fugacity of CO_2, fCO_2, measured with autonomous CARIOCA sensors [*Copin-Montégut et al.*, 2004; *Merlivat and Brault*, 1995] in 1995-1997 and 2013-2015, at two nearby locations in the northwestern Mediterranean Sea (Fig. 1). Using measured fCO_2, temperature (T) and salinity (S), we derive the other variables of the carbonate system (pH and DIC). The experimental setting is first described, and the recent data obtained over the 2013-2015 period are presented. Combined with the 1995-1997

measurements previously published [*Hood and Merlivat*, 2001], we estimate the decrease of pH and the increase of DIC. The results are discussed with respect to the contributions of the exchange with atmospheric CO_2, to the possible impact of vertical mixing and to recent estimates of the transport of anthropogenic carbon from the Atlantic Ocean over a 18-year period.

2 Material and methods

2.1-The BOUSSOLE and DYFAMED sites

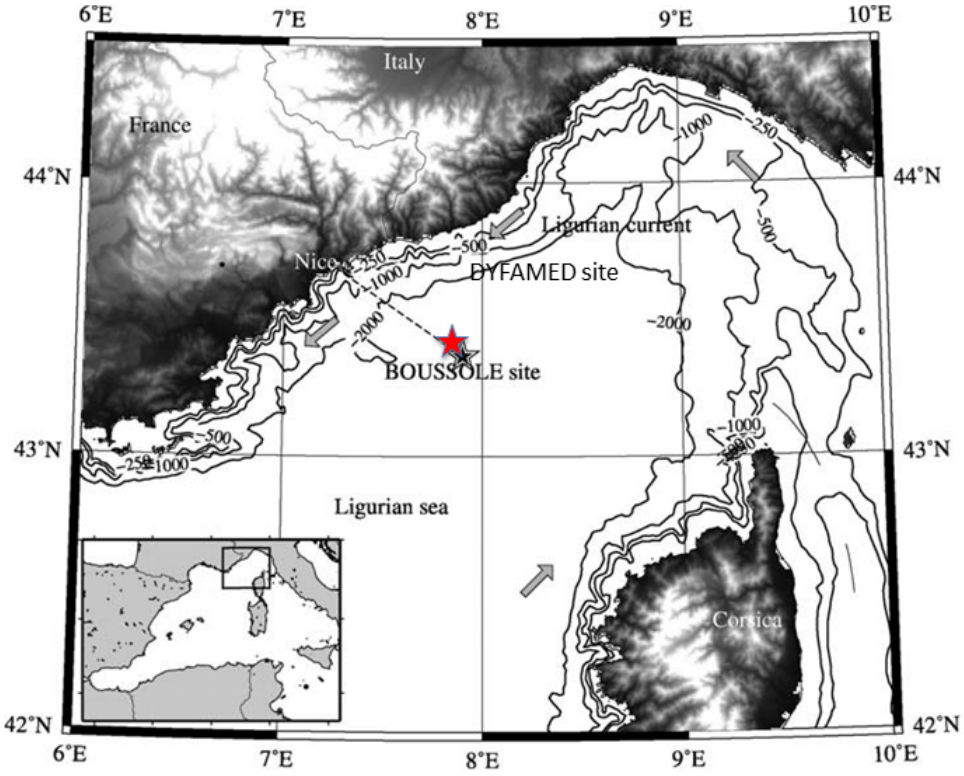

Fig.1. The area of the northwestern Mediterranean Sea showing the southern coast of France, the Island of Corsica, the main current branches (gray arrows), and the location of the DYFAMED site (43°25'N, 7°52'E, red star) (http://doi.org/10.17882/43749) and the BOUSSOLE buoy (43°22'N, 7°54'E, black star) in the Ligurian Sea.

Data collection was carried out at the BOUSSOLE site (43°22'N, 7°54'E) in 2013-2015 [*Antoine et al.*, 2008; *Antoine and others*, 2006] and at the DYFAMED site (43°25'N, 7°52'E) in 1995-1997 [*Marty et al.*, 2002]. These sites are 3 nautical miles apart, both located in the Ligurian Sea, one of the basins of the northwestern Mediterranean Sea (Fig.1). The water depth is ~2400 m. The prevailing ocean currents are usually weak (<20 cm s^{-1}), because these sites are in the central area of the cyclonic circulation that characterizes the Ligurian

Sea. The two sites surrounded by the permanent geostrophic Ligurian frontal jet flow are protected from coastal inputs [*Antoine et al.*, 2008; *Heimbürger et al.*, 2013; *Millot*, 1999]. Monthly cruises are carried out at the same location .

2.2- Analytical methods

At DYFAMED, fCO_2 measurements at 2 m were provided by an anchored floating buoy fitted with a CARIOCA sensor. At BOUSSOLE, measurements were carried out from a mooring normally dedicated to radiometry and optical measurements, and onto which two CARIOCA sensors were attached. Both monitored fCO_2 hourly at 3 and 10 m depth (although only one of the two depths was equipped with a functional sensor at some periods); S and T were monitored at the same two depths using a Seabird SBE 37-SM MicroCat instrument. The CARIOCA sensors were adapted to work under pressure in the water column. They were swapped about every 6 months, with serviced and calibrated instruments replacing those having been previously deployed. The accuracy of CARIOCA fCO_2 measurements by the spectrophotometric method based on the optical absorbance of a solution thymol blue diluted in seawater is estimated at 2 µatm during both periods. Hood and Merlivat [2001] have reported agreement between fCO_2 measured by CARIOCA buoys, similar to the one deployed at DYFAMED, with ship based measurements, during a number of field programs, with an accuracy of 2 µatm and a precision of 5 µatm .

At Boussole, newly designed fCO_2 sensors have been calibrated using in situ seawater samples taken at 5 and 10 m depth during the monthly servicing cruises to the mooring. The total alkalinity, Alk, and DIC of the samples were determined by potentiometric titration using a closed cell according to the method developed by [*Edmond*, 1970]. Certified Reference Materials (CRMs) supplied by Dr. A.G. Dickson (Scripps Institution of Oceanography, San Diego, USA) were used for calibration [*Dickson et al.*, 2007]. The accuracy is estimated at 3 µmol kg^{-1} for both DIC and Alk. fCO_2 is calculated using the dissociation constants of Mehrbach refitted by Dickson and Millero [*Dickson and Millero*, 1987; *Mehrbach et al.*, 1973] as recommended by Alvarez et al.[2014] for the Mediterranean Sea. Uncertainty in fCO_2 derived from an individual sample is expected to be on the order of 5 µatm [*Millero*, 2007]. About 8 samples have been used to calibrate each CARIOCA sensor so that the uncertainty of the absolute calibration of each fCO_2 CARIOCA sensor, is estimated at 1.8 µatm. In addition, we observe that the standard deviation of the difference between the CARIOCA fCO_2 and fCO_2 computed with the monthly discrete samples (Fig. 2b) is equal to 4.4 µatm, consistent with the expected precision on CARIOCA fCO_2 of 5 µatm. Alk and S of

the 56 samples taken at BOUSSOLE are linearly correlated according the following relationship :

$$Alk\ (\mu mol\ kg^{-1}) = 87.647\ S - 785.5 \qquad (1)$$

The standard deviation of the Alk data around the regression line is equal to 4.4 µmol kg^{-1} (r^2=0.89).

3 Results

3.1 The BOUSSOLE mooring (2013-2015) time series

Temperature and fCO_2 were measured from February 2013 to February 2016. All seasons were well represented, with missing data only in May-July 2013. For some periods, simultaneous measurements were made at 3 and 10 m depth (Fig. 2, a, b, c).

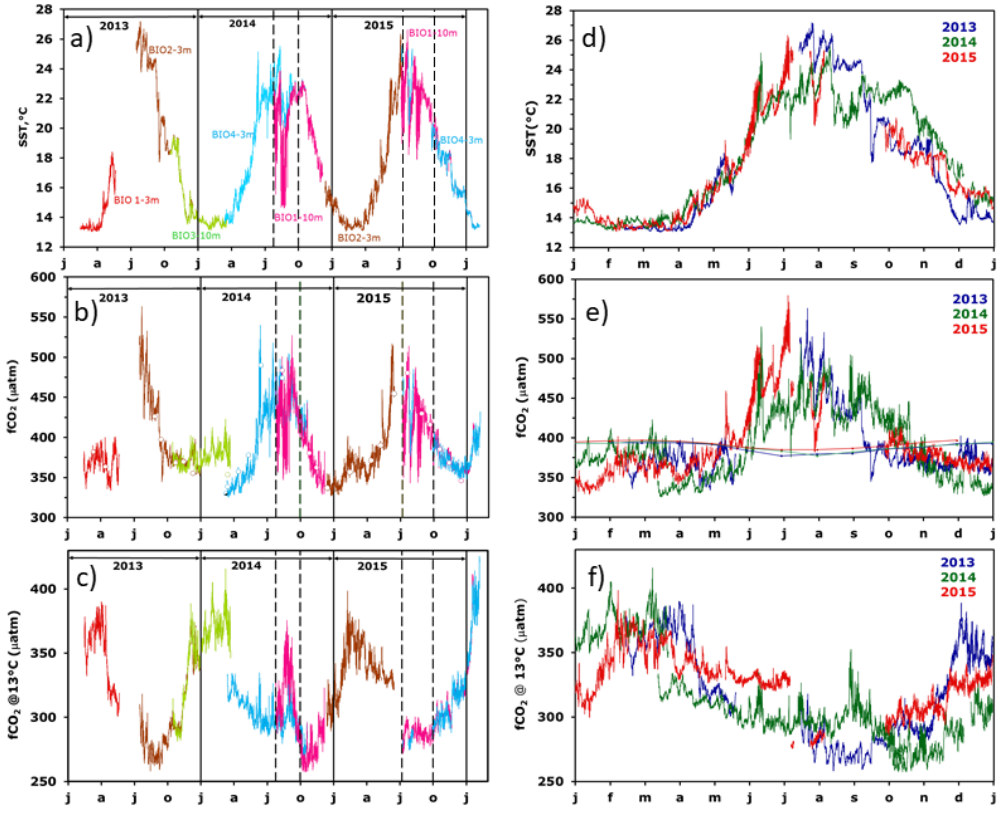

Fig.2. Interannual variability of CARIOCA data on the BOUSSOLE mooring: left column, as a function of time, right column as a function of months for a given year (blue, 2013, green, 2014, red, 2015). (a, d) T, (b, e), fCO_2, (c, f) fCO_2@13°C. On a, b, c, the dotted lines indicate the period affected by stratification and internal waves (July, 26 th to October 1st, 2014 and July, 8 th to October 1st, 2015). On 2(b), the open circles correspond to fCO_2 data derived from

DIC and alkalinity measurements of samples taken at 5 and 10 m. On 2(e), the thin lines indicate fCO_{2atm}. Note that the color code on (d), (e), (f) is different from (a), (b), (c).

The range of temperature (Fig. 2a) extends from 13°C in winter up to 27°C in summer, followed by progressive cooling in fall. The coldest temperature, 13°C, results from the winter vertical mixing with the deeper Levantine Intermediate Water, LIW, marked by extremes in temperature and salinity [*Copin-Montegut and Begovic*, 2002]. Temperature provides the main control of the seasonality of fCO_2, from 350 µatm to more than 550 µatm in summer 2013 (Fig. 2b). The fugacity of CO_2 in seawater is a function of temperature, DIC, alkalinity, salinity and dissolved nutrients. In the oligotrophic surface waters of the Mediterranean Sea, the effect of nutrients may be neglected. Temperature and DIC have the strongest influences. By normalizing fCO_2 to a constant temperature, the temperature effect can be removed and changes in fCO_2 resulting from changes in DIC can be more easily identified. Figure 2c shows the variability of fCO_2 normalized to the constant temperature of 13°C, (fCO_2@13), using the equation of Takahashi et al. [1993]. The underlying processes that govern the seasonal variability of fCO_2@13 are successively winter mixing, biological activity (organic matter formation and remineralization) and deepening of mixed layer in fall [*Begovic and Copin-Montegut*, 2002; *Hood and Merlivat*, 2001]. Biological processes account for the decline in fCO_2@13 observed from March-April to late summer; the ensuing increase of surface fCO_2@13 is associated with the deepening of the mixed layer in the fall or convection in winter as the vertical distribution of fCO_2@13 at DYFAMED shows a maximum in the 50-150 m layer where a large remineralization of organic matter occurs, the productive layer being mostly between 0 and 40 m [*Copin-Montegut and Begovic*, 2002]. The contribution of air-sea exchange is not significant [*Begovic and Copin-Montegut*, 2002]. Over the period 2013-2015, the air-sea CO_2 flux from the atmosphere to the ocean surface is equal to -0.45 mol m^{-2} yr^{-1}.

During summer 2014, large differences between measurements at 3 and 10 m were observed (Fig. 2, a, b, c between dashed lines). A detailed analysis of the temporal variability during that period underscores the role of inertial waves at the frequency of 17.4 hours that create the observed differences between the 2 depths of observations, the deeper waters being colder and enriched in fCO_2@13. Tempertature and fCO_2@13 variability is dominated by inertial waves. In particular, from 15 to 26 of August 2014, the difference in T between the two depths is as large as 7.6°C, and 5.1°C on average.

169 fCO_2 decreases on average by 32.7 μatm corresponding to an increase of fCO_2@13 equal
170 to 42.8 μatm.
171 The 2013-2015 seasonal and inter-annual variability of T, fCO_2 and fCO_2@13 is
172 illustrated on Fig. 2, d, e, f. The larger interannual changes in temperature (Fig.2, d) are
173 observed during summer, both at 3 m and 10 m depth, while over February and March, a
174 constant value of 13°C is observed as the result of vertical mixing with the LIW. A very
175 large inter-annual variability of fCO_2@13 is observed for T<14°C (Fig. 2,f). This is
176 associated with the winter mixing at the mooring site, which is highly variable from year
177 to year. Winter mixed-layer depth, MLD, varies between 50 and 160 m, at the top of the
178 LIW over the 2013-2015 period [*Coppola et al.*, 2016]. The variable depth of the winter
179 vertical mixing causes the difference in fCO_2@13 as fCO_2 increases with depth [*Copin-*
180 *Montegut and Begovic*, 2002]. The deepening of MLD is driven by episodic and intense
181 mixing processes characterized by a succession of events lasting several days, related to
182 atmospheric forcing [*Antoine et al.*, 2008] which lead to increase in fCO_2@13. Figure 2,e
183 illustrates the solubility control of the variability of fCO_2, as fCO2 increases when T
184 increases. Another cause of inter-annual variability of fCO_2 for T~14°C is the timing of
185 the spring increase of biological activity which differs by a month between years; for
186 instance, it happened at the beginning of April in 2013, T~15-16°C and by mid March in
187 2014, T~14°C. Another cause is the deepening of the mixed layer due to the fall cooling
188 which varies by a month between years.
189
190 **3.2** Decadal changes of hydrography
191 **3.2.1** Sea surface temperature changes
192 Monthly mean values of temperature have been computed for the two three-year periods,
193 1995-1997 and 2013-2015. In 1995-1997, fCO_2 and T at 2 m were measured with CARIOCA
194 sensors installed on a buoy at DYFAMED [*Hood and Merlivat*, 2001]. The mean annual
195 temperature of hourly CARIOCA data is equal to 18.21°C. For 2013-2015, temperature
196 measurements made on the BOUSSOLE mooring at 3 and 10 meters have been used. For the
197 April to September time interval, there are only data at 3m depth. In addition, temperature
198 data measured half hourly at 0.7 m at a nearby meteorological buoy (43°23'N, 7°50'E)
199 (http://www.meteo.shom.fr/real-time/html/DYFAMED.html) have been used (Fig.3d). Mean
200 annual temperatures are equal to 18.29°C and 17.97°C respectively, based on the
201 meteorological buoy and the BOUSSOLE mooring data. The two sets of data differ

202 essentially during July and August, with the temperatures at 3 m being colder than at 0.7 m,
203 indicating a thermal gradient between the two depths during summer. Therefore, for 2013-
204 2015, we select the mean annual value computed with the meteorological buoy, 18.29°C, as
205 better representing the sea surface. This value is close to 18.21°C computed for 1995-1997.
206 Then, no significant change of SST is found between the 2 decades, with a mean value equal
207 to 18.25°C.
208 **3.2.2** Sea surface salinity changes
209 The mean value of salinity and the standard error of the mean computed from 56 samples
210 taken at BOUSSOLE in 2013-2015 are respectively 38.19 and 0.02. In 1998-1999, ship
211 measurements of surface salinity were made during monthly cruises at the DYFAMED site
212 [*Copin-Montégut et al.*, 2004]. The mean salinity and the standard error of the mean of this
213 set of 19 data are respectively 38.21 and 0.03. Thus, there is no significant salinity change
214 between the two decades .
215
216 **3.3** Decadal changes of fCO_2@13
217 **3.3.1** Time series of fCO_2@13 in 1995-1997 and 2013-2015
218 The two time series of high frequency data were analyzed in order to quantify the change of
219 fCO_2@13 at the sea surface two decades apart. To account for the interannual seasonal
220 variability as well as irregular sampling, we performed an analysis of the change of fCO_2@13
221 as a function of SST (Fig. 3, a and b). For the 2013-2015 data set, we excluded summer data
222 measured at 10 m depth as they were not representative of the surface mixed layer due to a
223 strong stratification. Much larger fCO_2@13 values are observed at low temperature than at
224 high temperature, the decrease being similar for the two studied periods and strongly non
225 linear. As described in section 3.1, large values at low temperature result from mixing with
226 enriched deep waters during winter, and low values for 26°C-28°C temperatures occur at the
227 end of summer after biological drawdown of carbon. An increase of fCO_2@13 between the 2
228 periods is evident across the range of temperatures.

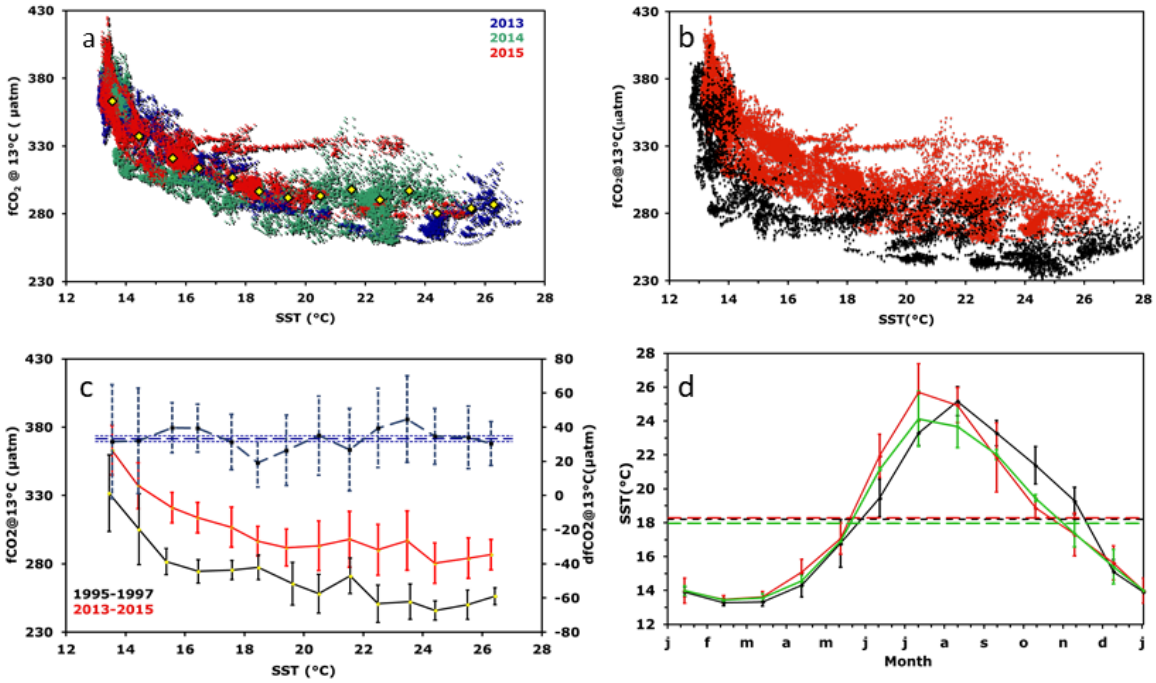

Fig.3. (a) fCO_2@13 as a function of temperature for hourly data in 2013, 2014 and 2015.The yellow dots indicate mean fCO_2@13. (b) as in (a) but for all hourly data in 1995-1997 (black) and in 2013-2015 (red). (c) as in (b), but for average values per 1°C interval (standard deviation as dotted line). The difference between the two periods is also displayed (dashed blue curve, scale on the right axis ; the mean difference over all SST is represented by the horizontal blue line). (d) Mean monthly sea surface temperature for 1993-1995 (black curve; CARIOCA sensors), 2013-2015 (green; CARIOCA sensors), 2013-2015 (red, meteorological buoy). Corresponding mean annual values are indicated by dotted lines.

3.3.2 Trend analysis and statistics

To quantify the change of fCO_2@13 between the two data sets, we proceed as follows: data are binned by 1°C temperature intervals, thereby removing any potential seasonal weighting, especially towards the 13-14°C winter months temperature. The measurements made in this temperature interval represent about 25% of the total number of data for both periods. For each of the fourteen 1°C step, the mean and standard deviation of hourly fCO_2@13 measurements are reported in Table 1 and on Fig. 3c. The mean temperature within each 1° step differ for the two periods as the distribution of individual measurements are not identical.

For both data sets, a monotonic relationship between fCO_2@13 and T is observed with correlation coefficients respectively equal to -0.861 and -0.857. The difference in fCO2@13 between the two periods, dfCO2@13, is derived in each temperature step, as the difference between column 2 and 6 of Table 1. The variability of this difference is estimated as the quadratic mean of the standard deviation in each time series. Both values are reported in Table 1, column 9 and 10, and on Fig. 3c. The distribution of each $dfCO_2$@13 values around the mean over all SST of $dfCO_2$@13 seems random and indicates no trend dependency with SST (Fig. 3c). This suggests that the processes which control the seasonal variation of fCO_2@13 at the sea surface have not changed over the last two decades.

We have estimated the uncertainties in the estimates of the difference $dfCO_2$@13 with 2 methods. Firstly, the arithmetic mean of $dfCO_2$@13 is equal to 33.17µatm, with a standard deviation, SD, and standard error, SE, respectively equal to 6.29 µatm and 1.68 µatm. A 95% confidence interval is thereby achieved within 1.96 SE, i.e 3.29 µatm. A second approach consists of computing a weighted average of the mean of $dfCO_2$@13. In this case, mean weighted value of $dfCO_2$@13 over the whole range of temperature is estimated, the weights being equal to the variance of $dfCO_2$@13 in each temperature step. It is equal to 32.70 µatm. The weighted SD, and the associated SE, of the 14 data points are respectively equal to 4.85 µatm and 1.30 µatm. A 95% confidence interval is achieved within 2.54 µatm. The difference between the two mean $dfCO_2$@13 estimates is 0.47 µatm, well below SE. In the following, we have chosen the former method.

Table 1:

Distribution of temperature, fCO2@13, and increase dfCO2@13 data binned by 1°C temperature interval for the 2 periods 1995-1997 and 2013-2015.

Time interval 1995-1997				Time interval 2013-2015				Temporal change	
T[1] °C	fCO2@13 µatm	N	standard deviation µatm	T[1] °C	fCO2@13 µatm	N	standard deviation µatm	dfCO2@13 µatm	standard deviation µatm
13.45	331.58	1212	28.09	13.55	363.14	6869	18.07	31.56	33.40
14.45	305.28	495	26.02	14.43	337.16	3270	16.65	31.87	30.89
15.37	281.54	447	9.62	15.57	321.10	3112	11.09	39.56	14.68
16.44	274.43	182	8.53	16.42	313.79	1818	11.09	39.36	13.99
17.58	275.54	190	7.04	17.56	306.83	1528	14.65	31.29	16.25
18.47	277.34	300	9.04	18.45	296.57	2621	10.95	19.23	14.20
19.62	265.43	342	15.58	19.41	291.84	1406	13.45	26.40	20.59
20.50	258.08	529	14.15	20.50	293.16	1135	18.21	35.08	23.06
21.56	271.15	239	12.98	21.54	297.96	1200	20.41	26.82	24.19
22.49	250.75	742	13.66	22.49	290.27	2385	18.57	39.52	23.05
23.57	252.22	320	13.00	23.47	296.92	747	21.77	44.70	25.36
24.41	245.85	506	7.08	24.40	280.44	959	14.82	34.59	16.43
25.50	250.06	215	10.77	25.53	284.05	456	14.81	33.99	18.31
26.42	256.29	279	6.24	26.29	286.71	249	11.23	30.42	12.85

3.4 Changes of seawater carbonate chemistry in surface waters

We estimated the DIC and pH changes related to the increase of fCO_2@13 measured at the sea surface 18 years apart, assuming a mean salinity equal to 38.2, a mean alkalinity equal to 2562.3 µmol kg^{-1} following equation (1), and a mean in situ temperature, T, equal to 18.25°C. The dissociation constants of Mehrbach refitted by Dickson and Millero [*Dickson and Millero*, 1987; *Mehrbach et al.*, 1973] were used. pH is calculated on the seawater scale.

The uncertainty of dfCO2@13, 3.3µatm, has been propagated to compute the combined uncertainty in dDIC and dpH_{SWS}. The uncertainties in the equilibrium constants are neglected in this propagation of uncertainties. Likewise, an implicit assumption is that there is no systematic error on DIC and pH_{SWS} derived from fCO2@13 between the two time periods; in particular, mean temperature and salinity remain the same (section 3.2). This is further discussed in section 4.1. We compute an increase of DIC, dDIC, equal to 25.2+/-2.7 µmol kg^{-1} (1.40+/-0.15 µmol $kg^{-1}yr^{-1}$) and the decrease of pH_{SWS}, dpH_{SWS} equal to -0.0397+/-0.0042 pH_{SWS} (-0.0022+/-0.0002 pH_{SWS} yr^{-1}) (Table 2).

Table 2

	d fCO_2* @ 13 µatm	d fCO_2* @ T µatm	d DIC* µmolkg^{-1}	d pH_{SWS}*** pH unit	$dfCO_2$@T annual µatm yr^{-1}	d DIC annual µmol$kg^{-1}yr^{-1}$	d pH_{SWS}*** annual pH unit yr^{-1}
sea surface	33.2 +/-3.3	41.4 +/-4.1	25.2 +/-2.7	-0.0397 +/-0.0042	2.30 +/-0.23	1.40 +/-0.15	-0.0022 +/- 0.0002
atmosphere Lampedusa data		34.3 +/-2.3	**20.8 +/-1.3		1.91 +/-0.13	1.15 +/-0.07	
$dfCO_2@T_{air}/dfCO_2@T_{sea}$		0.83 +/-0.10	0.83 +/-0.09				

T, mean annual temperature equal to 18.25°C

*, change from 1995-1997 to 2013-2015.

**, $dDIC_{ant}$

*** dpH_{SWS} computed at T

3.5 Changes in atmospheric and seawater fCO_2

The increase of atmospheric fCO_2 from 1995-1997 to 2013-2015 was computed from monthly atmospheric xCO_2 concentrations measured at the Lampedusa Island station (Italy) (35°31'N, 12°37'E) (http://ds.data.jma.go.jp/gmd/wdcgg/) (see equation 3 in [*Hood and Merlivat*, 2001]). Considering a mean annual in situ temperature equal to 18.25°C and an atmospheric pressure of 1 atm, we derived a mean atmospheric fCO_2 equal to 355.3+/-0.8 µatm for 1995-1997 and 389.6+/-0.9 µatm for 2013-2015, that is an increase of 34.3+/-2.3 µatm (95% confidence interval) (Table 2). At this temperature, the change of fCO_2 at the sea surface is 41.4+/-4.1 µatm. Thus the contribution of the increase in atmospheric CO_2 is

responsible for 84+/-5 % of the increase of fCO_2 measured in the surface waters. With the same salinity and alkalinity as previously, the corresponding change in surface DIC, assuming air-sea equilibrium, would be 20.8+/- 1.3 μmol kg^{-1} (Table 2).

4 Discussion

4.1 Time change of surface alkalinity

High frequency measurements of fCO_2 and temperature over 2 periods of 3 years, 2 decades apart, have allowed the computation of an increase of DIC equal to 25.1+/-2.3 μmol kg^{-1} assuming no change of alkalinity. In the range of salinity of the BOUSSOLE samples, 37.9 to 38.5, the alkalinity values computed with Eq (1) are larger than those predicted by the relationship established for the DYFAMED site, with a mean difference equal to 10+/-2 μmol kg^{-1} [*Copin-Montegut and Begovic*, 2002]. In both cases alkalinity measurements were made with a potentiometric method using certified reference material supplied by A.G. Dickson for calibration. It is difficult to identify the cause for a possible change of alkalinity between the 2 periods, 18 years apart, while no salinity change has been observed. At a coastal site 50 km away from DYFAMED, Kapsenberg et al. [2017] have measured an increase of alkalinity unrelated to salinity over the period from 2007 to 2015. They attribute it to changes in freshwater inputs from land. However, based on data from Coppola et al. [2016], alkalinity in the upper 50m at DYFAMED did not change significantly from 2007 through 2014 (3.204 μmol kg^{-1}, P=0.0794, r^{*2}=0.08). Thus, we cannot conclude on whether the difference observed at DYFAMED/BOUSSOLE between the two periods is real or an artifact of measurement techniques. As a sensitivity test, we compute the expected changes of DIC and pH from 1995-1997 to 2013-2015 for a mean alkalinity increase of 10 μmol kg^{-1}: we get annual changes, dDIC=+0.46 μmol kg^{-1} yr^{-1} and dpH=-0.0001 pH unit yr^{-1}, which are well below errors estimated in section 3.4. Hence, such a change in alkalinity does not significantly affect the increase of DIC and the decrease of pH shown in Table 2.

4.2 Drivers of the temporal change of DIC in surface waters

The increase in sea surface DIC from 1995-1997 to 2013-2015 is 25.2+/-2.7 μmol kg^{-1} (Table 2) whereas the expected contribution due to ocean uptake of anthropogenic CO_2 is 20.8+/-1.3 μmol kg^{-1}. In order to interpret the difference between these two values, we examine potential changes that may result from interannual variability in local physical and biological processes or anthropogenic carbon invasion from lateral advection of Atlantic waters.

4.2.1 Natural variability

Time series of the mixed layer depth, MLD, show a strong variability in winter at interannual scale. During the two periods, 1995-1997 and 2013-2015, the winter MLD never exceeded 220 m, whereas values over 300 m were observed in 1999 and especially in February and March 2006 with values close to 2000 m [*Coppola et al.*, 2016; *Pasqueron de Fommervault et al.*, 2015]. These episodes of strong and deep vertical mixing must have entrained DIC-rich LIW in the surface waters. This entrainment could be causing an increase in DIC between the 1995-1997 and 2013-2015 periods. Monthly surface samples collected at the Dyfamed time series station between 1998 and 2013 indicate an increasing DIC trend of 1.35 μmol kg^{-1} yr^{-1}. This value is known with great uncertainty ($r^2 = 0.05$) because of the large seasonal variability displayed in the monthly samples [*Gemayel et al.*, 2015]. Nevertheless, this value is closer to the trend we calculated between the two periods, 1993-1995 and 2013-2015 (1.40 μmol kg^{-1} yr^{-1}) than to the trend inferred from the atmospheric increase (1.15 μmol kg^{-1} yr^{-1}). On DYFAMED time series, we find no evidence that the strong increase in MLD observed during winters 1999 and especially 2006 resulted in a further increase in DIC.

The monthly cruises of the Dyfamed time-series study have also been analyzed in order to investigate the hydrological changes and some biological consequences over the period 1995-2007 [*Marty and Chiavérini*, 2010]. These authors show that extreme convective mixing events such as recorded in 1999 and 2006 are responsible for large increases in nutrient content in surface layers and conclude that the biological productivity is increasing especially during the 2003-2006 period, which could lead to a larger consumption of carbon, i.e. a decrease of DIC.

4.2.2 Anthropogenic carbon exchange through the Strait of Gibraltar.

The concentration of oceanic anthropogenic carbon, C_{ant}, is not a directly measurable quantity. To estimate it, several empirical methods have been developed. Flecha et al.[2012] computed the anthropogenic carbon inventory in the Gulf of Cadiz. They used observations made during a cruise in October 2008 throughout the oceanic area covered by the Gulf of Cadiz and the Strait of Gibraltar to estimate C_{ant} with 3 methods: ΔC* [*Gruber et al.*, 1996], TrOCA [*Touratier and Goyet*, 2004; *Touratier et al.*, 2007] , φC_T^0 [*Vazquez-Rodriguez et al.*, 2009]. In the 3 cases, their results indicate a net import of C_{ant} from the Atlantic towards the Mediterranean through Gibraltar.

Schneider et al. [2010], using the transit time distribution method applied to a dataset of a Mediterranean cruise in 2001, estimated a net anthropogenic carbon flux across the Strait of Gibraltar into the Mediterranean Sea of 3.5 Tg C yr^{-1}. Over the whole period from 1850 to 2001, this contribution of C_{ant} represents almost 10% of the total C_{ant} inventory of the

Mediterranean Sea. Accordingly, about 90% must have been taken directly by equilibrium with atmospheric CO_2. Based on a high-resolution regional model, Palmieri et al. [2015] computed the anthropogenic carbon storage in the Mediterranean basin. They concluded that 75% of the total storage of C_{ant} in the whole basin comes from the atmosphere and 25% from net transport from the Atlantic through the Strait of Gibraltar. The findings of these two studies support our estimated change of DIC of (17+/-10) % in addition to the direct contribution of air-sea exchange suggesting that it could result from the anthropogenic carbon input from the Atlantic Ocean towards the Mediterranean basin.

Huertas et al. [2009] and Schneider et al. [2010] report DIC_{ant} surface concentrations respectively equal to 65-70 µmol kg^{-1} at the Strait of Gibraltar in the years 2005-2007 and close to 65 µmol kg^{-1} in the western basin in 2001. We extrapolate these figures to the year 2014, assuming a mean increase rate of DIC equal to 1.4 µmol $kg^{-1}yr^{-1}$ as previously computed (Table 2). Taking into account the increase of DIC_{ant} equal to 25.2 µmol kg^{-1} between 1995-1997 and 2013-2015, we estimate that the contribution of the change of DIC_{ant} over the last 18 years represents ~30% of the total change since the beginning of the industrial period (t>~1800).

4.3 Long-term trends in surface DIC and pH

The annual changes of DIC and pH_{SWS} calculated between 1995-1997 and 2013-2015 are respectively equal to 1.40 +/-0.15 µmol kg^{-1} and -0.0022+/-0.0002. At the DYFAMED site, at 10 m, Marcellin Yao et al. [2016] studied the time variability of pH over 1995-2011, based on measurements of T, S, Alk and DIC sampled approximately once a month. They computed a mean annual decrease of -0.003 ± 0.001 pH units on the seawater scale that is not significantly different from our estimate. For the global surface ocean, Lauvset et al. [2015] have reported a mean rate of decrease of pH, -0.0018+/-0.0004 for 1991-2011. This value is also within the limits of uncertainty of the pH change computed in our study.

Bates et al. [2014] examined changes in surface seawater CO_2-carbonate chemistry at the locations of seven ocean CO_2 time series that have been gathering sustained observations from 15 to 30 years with monthly or seasonal sampling. Six stations are located in the Atlantic and Pacific oceans in a latitudinal band between 10° N and 68°N. The range of increasing and decreasing annual trends of DIC and pH extends from 0.93 +/-0.24 to 1.89 +/-0.45 µmol $kg^{-1}yr^{-1}$ and -0.0014+/-0.0005 to -0.0026+/-0.0006 respectively. The Revelle factor of surfaces waters vary from 9-10 in the low latitude to 12-15 in the subpolar time series sites, with higher Revelle factor values reflecting reduced capacity to absorb atmospheric CO_2. The

data show that the increase of DIC is not only controlled by the buffer capacity of the water but also compounding effects of changes in physical factors as strengthening of winter mixing or larger air-sea uptake [*Olafson et al.*, 2010].

The increase of DIC computed at DYFAMED is in the upper range of values reported at the other time series. A low Revelle factor, close to 10, characterizes the Mediterranean Sea because of its warm and high-alkalinity waters. Moreover, as the result of a relatively short deep water renewal time estimated to be 20-40 years in the western basin [*Schneider et al.*, 2010], the waters of the Mediterranean Sea have a relatively high capacity to absorb anthropogenic CO_2 from the atmosphere and transport it to depth.

The calculated decrease of pH in surface water at DYFAMED and in the global ocean are quite similar, despite the higher alkalinity of the Mediterranean Sea. Thermodynamic equilibrium calculations have highlighted the alkalinity effect on the anthropogenic acidification of the Mediterranean Sea [*Palmiéri et al.*, 2015]. Their results show that, notwithstanding a higher total alkalinity, the average anthropogenic change in surface pH of the Mediterranean Sea does not differ significantly from that of the global average ocean.

5 Conclusion

High-frequency ocean fCO_2 measurements made by CARIOCA sensors have been used to calculate trends in fCO_2, DIC and pH over a period of two decades notwithstanding a short-time and natural seasonal variability of these properties at the sea surface. We have estimated a large change of sea surface carbonate chemistry, an increase of DIC and a decrease of pH. The computed increase of DIC is larger than the change expected from chemical equilibrium with atmospheric CO_2.This could be the result of a strong interannual variability of the winter mixing as observed between the two periods 1993-1995 and 2013-2015. Likewise, our results support modeling work and analysis of vertical profiles measurements that suggest that the Atlantic Ocean contributes a substantial amount of anthropogenic carbon to the Mediterranean basin, (17+/-10) %, which lies between the estimates of 10% by Schneider et al. [2010] and 25% by Palmieri et al. [2015].

Data availability: Time series data from Dyfamed (19951997) are available in the SOCAT v3 database. Boussole data (2013-2015) will be available in SOCAT v6.

Acknowledgments

Seawater samples were analyzed for DIC and Alk by the SNAPO-CO_2 at LOCEAN in Paris.

457 The CO2Sys toolbox of [*Pierrot et al.*, 2006] has been used for the calculations of DIC and
458 pH. The adaptation of CARIOCA sensors to high pressure has been supported by the BIO-
459 optics and CARbon EXperiment (BIOCAREX) project, funded by the Agence Nationale de la
460 Recherche (ANR,Paris). We are grateful for helpful comments from Gilles Reverdin and the
461 reviewers on the manuscript. Many thanks to Laurent Coppola who kindly provided
462 additional MLD data at Dyfamed.
463

464 **References**

465 Alvarez, M., H. Sanleon-Bartolome, T. Tanhua, L. Mintrop, A. Luchetta, C. Cantoni,
466 K. Schröder, and G. Civitarese (2014), The CO2 system in the Mediterranean Sea: a basin
467 wide perpestive, *Ocean Sci.,*, *10*, 69-92.

468 Antoine, D., F. d'Ortenzio, S. B. Hooker, G. Bécu, B. Gentili, D. Tailliez, and A. J.
469 Scott (2008), Assessment of uncertainty in the ocean reflectance determined by three satellite
470 ocean color sensors (MERIS, SeaWiFS and MODIS-A) at an offshore site in the
471 Mediterranean Sea (BOUSSOLE project), *Journal of Geophysical Research*, *113*(C7).

472 Antoine., and others (2006), BOUSSOLE: A Joint CNRS-INSU,ESA, CNES and
473 NASA ocean color calibration and validation activity., *NASA Tech. Memo. 2006-214147.*

474 Bakker, D. C. E., et al. (2014), An update to the Surface Ocean CO₂
475 Atlas (SOCAT version 2), *Earth Syst. Sci. Data*, *6*(1), 69-90.

476 Bates, N., Y. Astor, M. Church, K. Currie, J. Dore, M. Gonaález-Dávila, L. Lorenzoni,
477 F. Muller-Karger, J. Olafsson, and M. Santa-Casiano (2014), A Time-Series View of
478 Changing Ocean Chemistry Due to Ocean Uptake of Anthropogenic CO2 and Ocean
479 Acidification, *Oceanography*, *27*(1), 126-141.

480 Begovic , M., and C. Copin-Montegut (2002), Processes controlling annual variations
481 in the partial pressure of fCO2 in surface waters of the central northwestern Mediterranean
482 sea (Dyfamed site), *Deep-Sea Research II*, *49*, 2031-2047.

483 Chen, G. T., and F. J. Millero (1979), Gradual increase of oceanic CO2, *Nature*, *277*,
484 205-206.

485 Copin-Montegut, C., and M. Begovic (2002), Distributions of carbonate properties and
486 oxygen along the water column (0–2000 m) in the central part of the NW Mediterranean Sea
487 (Dyfamed site): influence of winter vertical mixing on air–sea CO2 and O2 exchanges, *Deep-*
488 *Sea Research II 49*, 2049-2066.

Copin-Montégut, C., M. Bégovic, and L. Merlivat (2004), Variability of the partial pressure of CO2 on diel to annual time scales in the Northwestern Mediterranean Sea, *Mar Chem*, *85*(3-4), 169-189.

Coppola, L., E. Diamond Riquier, and T. Carval (2016), Dyfamed observatory data, *SEANOE*.

Dickson, A. G., and F. J. Millero (1987), A comparison of the equilibrium constants for the dissociation of carbonic acid in seawater media, *Deep Sea Research Part A. Oceanographic Research Papers*, *34*(10), 1733-1743.

Dickson, A. G., C. L. Sabine, and J. R. Christian (2007), Guide to best practices for ocean CO2 measurements, *PICES Spec.Publ.3*, 176.

Edmond, J. M. (1970), High precision determination of titration alkalinity and total carbon dioxide content of seawater by potentiometric titration, *Deep Sea research 17*(4), 737-750.

Flecha, S., F. F. Pérez, G. Navarro, J. Ruiz, I. Olivé, S. Rodríguez-Gálvez, E. Costas, and I. E. Huertas (2012), Anthropogenic carbon inventory in the Gulf of Cádiz, *Journal of Marine Systems*, *92*(1), 67-75.

Gattuso, J.-P., and L. Hansson (2011), Ocean Acidification, *Oxford University Press*, 352 pp.

Gemayel, E., A. E. R. Hassoun, M. A. Benallal, C. Goyet, P. Rivaro, M. Abboud-Abi Saab, E. Krasakopoulou, F. Touratier, and P. Ziveri (2015), Climatological variations of total alkalinity and total dissolved inorganic carbon in the Mediterranean Sea surface waters, *Earth System Dynamics*, *6*(2), 789-800.

Gruber, N., J. L. Sarmiento, and T. F. Stocker (1996), An improved method for detecting anthropogenic CO2 in the oceans, *Global Biogeochem Cy*, *10*, 809-837.

Heimbürger, L.-E., H. Lavigne, C. Migon, F. D'Ortenzio, C. Estournel, L. Coppola, and J.-C. Miquel (2013), Temporal variability of vertical export flux at the DYFAMED time-series station (Northwestern Mediterranean Sea), *Progress In Oceanography*, *119*, 59-67.

Hood, E. M., and L. Merlivat (2001), Annual and interannual variations of fCO2 in the northwestern Mediterranean Sea:Results from hourly measurements made by CARIOCA buoys, 1995-1997, *J Mar Res*, *59*, 113-131.

Huertas, I. E., A. F. Ríos, J. García-Lafuente, A. Makaoui, S. ` Rodríguez-Gálvez, A. Sánchez-Román, A. Orbi, J. Ruíz, and F. F. and Pérez (2009), Anthropogenic and natural CO2 exchange through the Strait of Gibraltar, *Biogeosciences*, *6*, 647-662.

Kapsenberg, L., S. Alliouane, F. Gazeau, L. Mousseau, and J.-P. Gattuso (2017), Coastal ocean acidification and increasing total alkalinity in the northwestern Mediterranean Sea, *Ocean Science*, *13*(3), 411-426.

Lauvset, S. K., N. Gruber, P. Landschützer, A. Olsen, and J. Tjiputra (2015), Trends and drivers in global surface ocean pH over the past 3 decades, *Biogeosciences*, *12*(5), 1285-1298.

Marcellin Yao, K., O. Marcou, C. Goyet, V. Guglielmi, F. Touratier, and J.-P. Savy (2016), Time variability of the north-western Mediterranean Sea pH over 1995–2011, *Marine Environmental Research*, *116*, 51-60.

Marty, J. C., and J. Chiavérini (2010), Hydrological changes in the Ligurian Sea (NW Mediterranean, DYFAMED site) during 1995–2007 and biogeochemical consequences, *Biogeosciences*, *7*(7), 2117-2128.

Marty, J. C., J. Chiaverini, M. Pizay, D.,, and B. Avril (2002), Seasonal and interannual dynamics of nutrients and phytoplankton pigments in the western Mediterranean Sea at the DYFAMED time-series station (1991–1999), *Deep-Sea Research II*, *49*, 1965-1985.

McKinley, G. A., A. R. Fay, T. Takahashi , and N. Metzl (2011), Convergence of atmospheric and North Atlantic carbon dioxide trends on multidecadal timescales, *Nature Geoscience*, *4*, 606-610.

Mehrbach, C., C. H. Culberson, J. E. Hawley, and R. M. Pytkowicx (1973), Measurement of the apparent dissociation constants of carbonic acid in seawater at atmospheric pressure, *Limnol Oceanogr*, *18*(6), 897-907.

Merlivat, L., and P. Brault (1995), CARIOCA BUOY: Carbon Dioxide Monitor, *Sea Technol*(October), 23-30.

Millero, F. J. (2007), The marine inorganic carbon cycle, *Chemical reviews*, *107*(2), 308-341.

Millot (1999), Circulation in the Western Mediterranean Sea, *Journal of Marine Systems*, *20*, 423–442.

Olafson, J., S. Olafsdottir, A. Benoit-Cattin, and T. Takahashi (2010), The Irminger Sea and the Iceland Sea time series measurements of sea water carbon and nutrient chemistry 1983-2008, *Earth Syst. Sci. Data*, *2*, 99-104.

Palmiéri, J., J. C. Orr, J. C. Dutay, K. Béranger, A. Schneider, J. Beuvier, and S. Somot (2015), Simulated anthropogenic CO2 storage and acidification of the Mediterranean Sea, *Biogeosciences*, *12*(3), 781-802.

556 Pasqueron de Fommervault, O., C. Migon, F. D′Ortenzio, M. Ribera d'Alcalà, and L.
557 Coppola (2015), Temporal variability of nutrient concentrations in the northwestern
558 Mediterranean sea (DYFAMED time-series station), *Deep Sea Research Part I:*
559 *Oceanographic Research Papers*, *100*, 1-12.
560 Pierrot, D., E. Lewis, and D. W. R. Wallace (2006), MS excel program developed for
561 CO2 system calculations, *In: Carbon Dioxide Information Analysis Center (ed.O.R.N.L.).*
562 *US.Department of Energy, Oak Ridge, TN.*
563 Sabine, C. L., R. A. Feely, F. J. Millero, A. G. Dickson, C. Langdon, S. Mecking, and
564 D. Greeley (2008), Decadal changes in Pacific carbon, *J.Geophys.Res.,*, *113*(C07021).
565 Schneider, A., T. Tanhua, A. Körtzinger, and D. W. R. Wallace (2010), High
566 anthropogenic carbon content in the eastern Mediterranean, *Journal of Geophysical Research*,
567 *115*(C12).
568 Takahashi , T., J. Olafson, J. G. Goddard, D. W. Chipman , and G. Sutherland (1993),
569 Seasonal variations of CO2 and nutrients in the high-latitude surface oceans:a comparative
570 study, *Global Biogeochem Cy*, *7*(4), 843-878.
571 Touratier, F., and C. Goyet (2004), Applying the new TrOCA approach to assess the
572 distribution of anthropogenic CO2 in the Atlantic Ocean, *Journal of Marine Systems*, *46*(1-4),
573 181-197.
574 Touratier, F., and C. Goyet (2009), Decadal evolution of anthropogenic CO2 in the
575 northwestern Mediterranean Sea from the mid-1990s to the mid-2000s, *Deep Sea Research*
576 *Part I: Oceanographic Research Papers*, *56*(10), 1708-1716.
577 Touratier, F., L. Azouzi, and C. Goyet (2007), CFC-11, ?14C and3H tracers as a
578 means to assess anthropogenic CO2concentrations in the ocean, *Tellus B*, *59*(2), 318-325.
579 Vazquez-Rodriguez, M., X. A. Padin, A. F. Rios, R. G. J. Bellerby, and Perez.F.F.
580 (2009), An upgraded carbon-based method to estimate the anthropogenic fraction of dissolved
581 CO2 in the Atlantic Ocean, *Biogeosciences Discussions*, *6*, 4527-4571.
582 Woosley, R. J., F. J. Millero, and R. Wanninkhof (2016), Rapid anthropogenic
583 changes in CO2and pH in the Atlantic Ocean: 2003-2014, *Global Biogeochem Cy*, *30*(1), 70-
584 90.
585
586

586 Table 1:

587

588 Distribution of temperature, fCO_2@13, and increase $dfCO_2$@13 data binned by 1°C

589 temperature interval for the 2 periods 1995-1997 and 2013-2015 .

590

591

Time interval 1995-1997				Time interval 2013-2015				Temporal change	
T[1] °C	fCO2@13 µatm	N	standard deviation µatm	T[1] °C	fCO2@13 µatm	N	standard deviation µatm	dfCO2@13 µatm	standard deviation µatm
13.45	331.58	1212	28.09	13.55	363.14	6869	18.07	31.56	33.40
14.45	305.28	495	26.02	14.43	337.16	3270	16.65	31.87	30.89
15.37	281.54	447	9.62	15.57	321.10	3112	11.09	39.56	14.68
16.44	274.43	182	8.53	16.42	313.79	1818	11.09	39.36	13.99
17.58	275.54	190	7.04	17.56	306.83	1528	14.65	31.29	16.25
18.47	277.34	300	9.04	18.45	296.57	2621	10.95	19.23	14.20
19.62	265.43	342	15.58	19.41	291.84	1406	13.45	26.40	20.59
20.50	258.08	529	14.15	20.50	293.16	1135	18.21	35.08	23.06
21.56	271.15	239	12.98	21.54	297.96	1200	20.41	26.82	24.19
22.49	250.75	742	13.66	22.49	290.27	2385	18.57	39.52	23.05
23.57	252.22	320	13.00	23.47	296.92	747	21.77	44.70	25.36
24.41	245.85	506	7.08	24.40	280.44	959	14.82	34.59	16.43
25.50	250.06	215	10.77	25.53	284.05	456	14.81	33.99	18.31
26.42	256.29	279	6.24	26.29	286.71	249	11.23	30.42	12.85

592

593

594

595

596

597

598

Table 2

Seasonally detrended long term and annual trends of seawater carbonate chemistry and atmosphere composition.

	d fCO_2* @ 13 µatm	d fCO_2* @ T µatm	d DIC* µmolkg^{-1}	d pH_{SWS}*** pH unit	$dfCO_2$@T annual µatm yr^{-1}	d DIC annual µmolkg^{1}yr^{1}	d pH_{SWS}*** annual pH unit yr^{1}
sea surface	33.2 +/-3.3	41.4 +/-4.1	25.2 +/-2.7	-0.0397 +/-0.0042	2.30 +/-0.23	1.40 +/-0.15	-0.0022 +/-0.0002
atmosphere Lampedusa data		34.3 +/-2.3	**20.8 +/-1.3		1.91 +/-0.13	1.15 +/-0.07	
$dfCO_2@T_{air}/dfCO_2@T_{sea}$		0.83 +/-0.10	0.83 +/-0.09				

T,mean annual temperature equal to 18.25°C

*, Change from 1995-1997 to 2013-2015.

**, $dDIC_{ant}$

***, dpH_{SWS} computed at T

Fig.1. The area of the northwestern Mediterranean Sea showing the southern coast of France, the Island of Corsica, the main current branches (gray arrows), and the location of the DYFAMED site (43°25'N, 7°52'E, red star) (http://doi.org/10.17882/43749) and the BOUSSOLE buoy (43°22'N, 7°54'E, black star) in the Ligurian Sea.

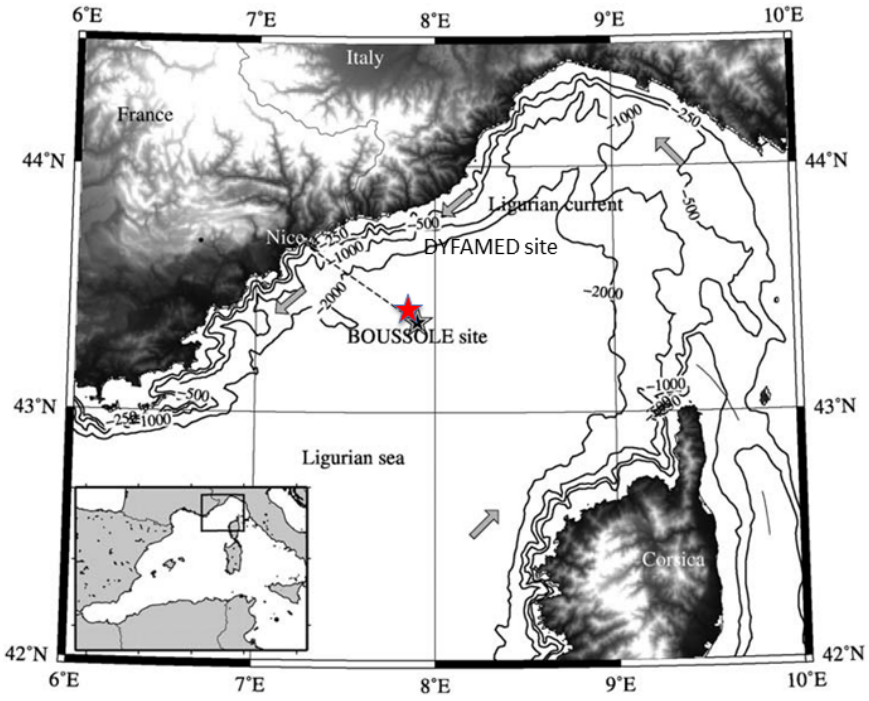

Fig.2. Interannual variability of CARIOCA data on the BOUSSOLE mooring: left column, as a function of time, right column as a function of months for a given year (blue, 2013, green, 2014, red, 2015). (a, d) T, (b, e), fCO_2, (c, f) fCO_2@13°C. On a, b, c, the dotted lines indicate the period affected by stratification and internal waves (July, 26 th to October 1st, 2014 and July, 8 th to October 1st, 2015). On 2(b), the open circles correspond to fCO_2 data derived from DIC and alkalinity measurements of samples taken at 5 and 10 m. On 2(e), the thin lines indicate fCO_{2atm}. Note that the color code on (d), (e), (f) is different from (a), (b), (c).

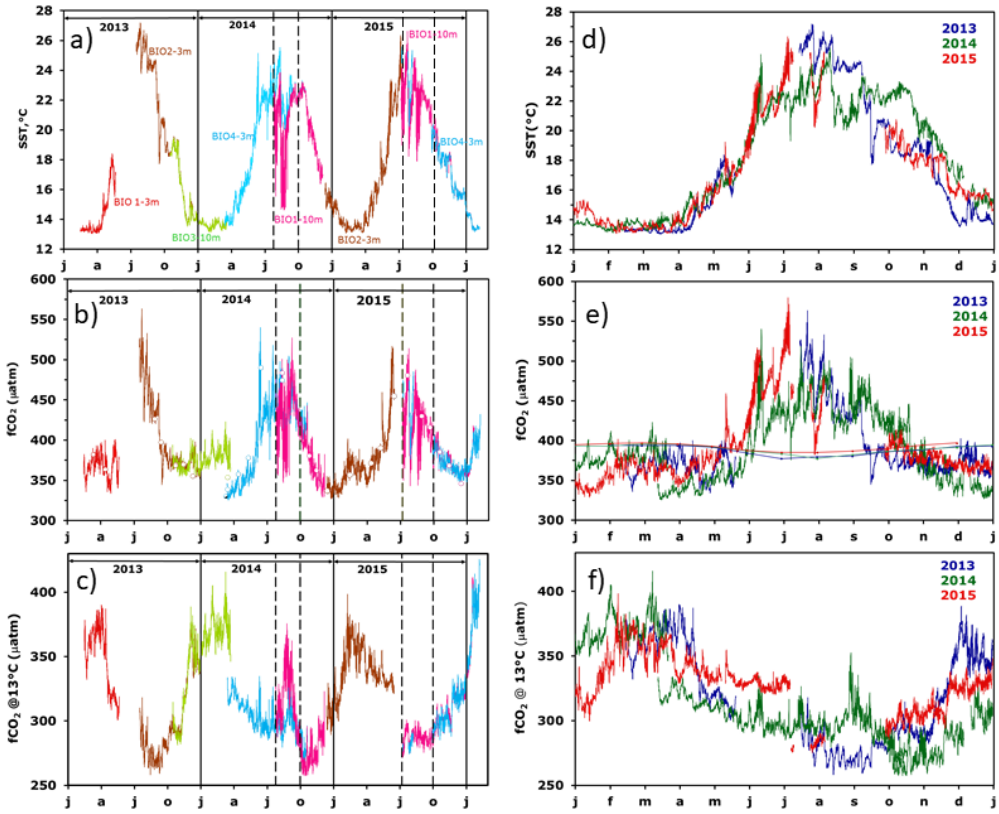

Fig.3. (a) fCO_2@13 as a function of temperature for hourly data in 2013, 2014 and 2015.The yellow dots indicate mean fCO_2@13. (b) as in (a) but for all hourly data in 1995-1997 (black) and in 2013-2015 (red). (c) as in (b), but for average values per 1°C interval (standard deviation as dotted line). The difference between the two periods is also displayed (dashed blue curve, scale on the right axis; the mean difference over all SST is represented by the horizontal blue line). (d) Mean monthly sea surface temperature for 1993-1995 (black curve; CARIOCA sensors), 2013-2015 (green; CARIOCA sensors), 2013-2015 (red, meteorological buoy). Corresponding mean annual values are indicated by dotted lines.

.